Specific amino-acid residues in the N-terminus and TM3 implicated in channel function and oligomerization compatibility of connexin43

Valérie Lagrée[1,*], Karin Brunschwig[1,‡], Patricia Lopez[1], Norton B. Gilula[1,§], Gabriele Richard[2] and Matthias M. Falk[1,¶]

1Department of Cell Biology, The Scripps Research Institute, 10550 North Torrey Pines Road, La Jolla, CA 92037, USA
[2]Department of Dermatology and Cutaneous Biology, and Jefferson Institute of Molecular Medicine, Thomas Jefferson University, Philadelphia, PA, USA

*Present address: Université de Bordeaux I, Pôle Biologie Cellulaire et Moléculaire, Institut Européen de Chimie et Biologie, Avenue des Facultés, 33405 Talence Cedex, France
‡Present address: Department of Biology, University of Fribourg, Perolles, Ch-1700 Fribourg, Switzerland
§Deceased September 2000
¶Author for correspondence (e-mail: mfalk@scripps.edu)

Accepted 9 April 2003
Journal of Cell Science 116, 3189-3201 © 2003 The Company of Biologists Ltd
doi:10.1242/jcs.00604

Summary

To identify signals that convey connexin oligomerization compatibility, we have aligned amino-acid sequences of α and β group connexins (Cx) and compared the physico-chemical properties of each homologous amino-acid residue. Four positions were identified that consistently differed between α and β-type connexins; two are located in the N-terminal domain (P1 and P2, corresponding to residues 12 and 13 of the Cx43 sequence), and two in the third trans-membrane-spanning domain TM3 (P3 and P4, corresponding to residues 152 and 153 of the Cx43 sequence). Replacement of each of these residues in Cx43 (an α-type connexin) with the corresponding residues of Cx32 (a β-type connexin) resulted in the assembly of all variants into gap junctions; however, only the P4 variant was functional, as indicated by lucifer yellow dye transfer assays. The other three variants exerted a moderate to severe dose-dependent, dominant-negative effect on co-expressed wild-type (wt) Cx43 channel activity. Moreover, a significant dose-dependent, trans-dominant inhibition of channel activity was observed when either one of the N-terminal variants was co-expressed with wt Cx32. Assembly analyses indicated that dominant and trans-dominant inhibitory effects appeared to be based on the oligomerization of wt and variant connexins into mixed connexons. Interestingly, the identified N-terminal amino acids coincide with the position of naturally occurring, disease-causing missense mutations of several β-connexin genes (*Cx26, Cx30, Cx31, Cx32*). Our results demonstrate that three of the identified discriminative amino-acid residues (positions 12, 13 and 152) are crucial for Cx43 channel function and suggest that the N-terminal amino-acid residues at position 12/13 are involved in the oligomerization compatibility of α and β connexins.

Key words: Gap junction diseases, Gap junctions, Green fluorescent protein, Membrane channels, Oligomeric proteins, Connexin subunit assembly

Introduction

Gap junctions are tightly packed arrays of membrane channels that mediate intercellular communication in multicellular organisms (reviewed in Bruzzone et al., 1996; Goodenough et al., 1996; Kumar and Gilula, 1996). They provide a pathway for the direct passage of ions, secondary messengers and other molecules up to 1 kDa in size. Communication via gap junctions mediates diverse cellular processes, such as coordination of metabolic activities, propagation of electrical signals, as well as regulation of cell growth, tissue and organ development (reviewed in Simon and Goodenough, 1998; White and Paul, 1999). Recently, mutations in connexin genes encoding gap junction proteins have been associated with several human diseases, such as X-linked Charcot-Marie-Tooth neuropathy, tumorigenesis, cataractogenesis, sensorineural deafness and a number of distinct skin disorders (reviewed in Kelsell et al., 2001; Richard, 2001).

A gap junction channel is formed by integral membrane proteins, termed connexins (Cx), which oligomerize into a hexameric hemichannel, termed a connexon. Two connexons, each provided by one of two neighboring cells, dock to form a functional intercellular channel. Connexins are polytopic membrane proteins spanning the membrane four times. The N- and C-termini, as well as the loop between the second and third transmembrane-spanning domains (TM2, TM3), are located in the cytoplasm. The two conserved sequence domains that connect the trans-membrane domains form the extracellular loops E1 and E2. They were implicated in voltage gating (Rubin et al., 1992), and connexon compatibility, which leads to the docking of connexons onto complete homo- and hetero-typic gap junction channels (Dahl et al., 1992; White and Bruzzone, 1996). The essential features of the trans-membrane topology of connexins, determined previously by biochemical approaches (Falk and Gilula, 1998; Falk et al., 1994; Hertzberg et al., 1988; Milks et al., 1988; Zimmer et al., 1987), was confirmed by the cryo-crystallographic structural analysis of Cx43 (α_1) gap junction channels (Unger et al., 1999).

Twenty different connexins have been identified in humans, and many homologues exist in other species. They have been divided phylogenetically into subgroups with α (also termed group 2) and β (also termed group 1) connexins being the two major representatives (six and seven members in humans, respectively); however, connexin classification and definition of subgroup-specific criteria is still under debate (reviewed in Bennett et al., 1994; Kumar and Gilula, 1992; Willecke, 2002). Connexins are expressed in a tissue-specific manner and most cell types express more than one connexin isoform. Therefore, not only are homo-oligomeric connexons consisting of one connexin isoform, but also hetero-oligomeric connexons consisting of different isoforms likely to exist in vivo and considerably increase the number of different gap junction channel types (Brink et al., 1997; Falk et al., 1997; He et al., 1999; Jiang and Goodenough, 1996; Konig and Zampighi, 1995; Stauffer, 1995; Wang and Peracchia, 1998). When we examined the oligomerization behavior of different connexin isoforms, we found that not all connexins oligomerized with each other to form hetero-oligomeric connexons (Falk et al., 1997). This observation prompted us to suggest that connexin isoform interaction is selective and restricts the possible number of hetero-oligomeric connexons (Falk et al., 1997). Indeed, all hetero-oligomeric connexons reported to date are composed of two members of the same subgroup. For instance, Cx43 has been shown to hetero-oligomerize with Cx37 (Brink et al., 1997), Cx40 (Cottrell and Burt, 2001; He et al., 1999; Valiunas et al., 2001) and Cx46 (Berthoud et al., 2001; Das Sarma et al., 2001) (all α-types) but not with Cx32 (Das Sarma et al., 2001; Falk et al., 1997) (a β-type). Furthermore, Cx46 has been reported to hetero-oligomerize with Cx50 (Jiang and Goodenough, 1996) (both α-types), whereas Cx32 can hetero-oligomerize with Cx26 (Locke et al., 2000; Stauffer, 1995) (both β-types). Connexin composition alters the properties and specificity of gap junction channels towards size, charge and characteristics of permeate molecules (Bevans et al., 1998; Goldberg et al., 1999; Steinberg et al., 1994; Veenstra, 1996), suggesting that the different channel subtypes are specifically adapted to precisely regulate the function of the cells in which they are expressed. In analogy, many different subunits of vertebrate ligand- and voltage-gated ion channels have been characterized that also can oligomerize into many different hetero-oligomeric channel subtypes (reviewed in Green and Millar, 1995). However, as with connexins, the number of possible combinations far exceeds the actual number of different ion channel subtypes that are assembled in vivo.

In search of signals that regulate the interaction of connexins, we aligned α and β connexin protein sequences and compared the physico-chemical properties at all positions. We identified four discriminatory residues. To determine whether these four residues convey connexin-specific compatibility, we exchanged each of these residues in Cx43 (an α type) with the corresponding residue of Cx32 (a β type). The Cx43 amino-acid exchange variants were expressed as GFP-tagged fusion proteins and their assembly, intracellular trafficking and lucifer yellow (LY) dye transfer capability was analyzed. In addition, we co-expressed each Cx43 variant with wild-type (wt) Cx43 or Cx32 and determined their ability to interact with and inhibit the function of co-expressed wild-type connexins.

Materials and Methods

Connexin sequence alignment

Connexin amino-acid sequences were aligned using the CLUSTAL W algorithm of the OMIGA 1.1 sequence analysis package (Oxford Molecular Group Inc., Oxford, UK, www.omiga.com). Sequences were extracted using the ExPASy Molecular Biology Server (http://www.expasy.org) of the Swiss Institute of Bioinformatics (SIB). Connexins and their SWISS-PROT and TrEMBL accession numbers are as follows: hCx43 (P17302), mCx43 (P23242), hCx46 (Q9Y6H8), mCx46 (Q64448), hCx37 (P35212), mCx37 (P28235), hCx40 (P36382), mCx40 (Q01231), hCx62 (Q969M2), mCx57 (Q9WUS4), hCx50 (P48165), mCx50 (P28236), hCx32 (P08034), mCx32 (P28230), hCx26 (P29033), mCx26 (Q00977), hCx31 (O75712), mCx31 (P28231), hCx31.1 (O95377), mCx31.1 (Q02739), hCx30.3 (Q9NTQ9), mCx30.3 (Q02738), hCx30 (O95452) and mCx30 (P70689).

Plasmid construction and site-directed mutagenesis

The plasmid containing the Cx43-GFP fusion protein was constructed by inserting the cDNA encoding the entire coding sequence except its authentic stop codon of rat Cx43 into the *Eco*RI/*Kpn*I cloning sites of the expression vector pEGFPN1 (Clontech Laboratories, Palo Alto, CA USA). The resulting construct consisted of the Cx43 sequence in frame with the EGFP coding sequence separated by a 12 amino acid linker sequence. Four different single and one double amino-acid substitution were introduced into the Cx43 cDNA using a Quickchange site-directed mutagenesis kit (Stratagene, La Jolla, CA, USA) according to the manufacturer's instructions. The forward primers corresponding to each mutation were as follows. The exchanged nucleotides are given in bold, and the mutated codons are underlined.

D12S: 5′-CTTGGGGAAGCTTCTG**AGT**AAGGTCCAAGCCTA-C-3′

K13G: 5′-GGGGAAGCTTCTGGAC**GGC**GTCCAAGCCTACT-CC-3′

DK12/13SG: 5′-CTTGGGGAAGCTTCTG**AGTGGC**GTCCAA-GCCTACTCC-3′

L152W: 5′-GAGGGGCGGCTTG**TGG**AGAACCTACATCATC-AGC-3′

R153W: 5′-GAGGGGCGGCTTGCTG**TGG**ACCTACATCATCA-GC-3′

All Cx43 constructs were verified by automated DNA sequencing.

Cells, cell culture and transfection conditions

Baby Hamster Kidney cells (BHK-21, ATCC CCL10) were used throughout this study. Stably transfected BHK cells expressing Cx43 and Cx32 (designated BHK-Cx43 and BHK-Cx32), respectively, were constructed as described previously (Kumar et al., 1995). In these cell lines the Cx cDNAs are under the control of an inducible metallothionine promotor that allows the expression of variable amounts of Cx protein after induction with different amounts of zinc acetate. Wild-type BHK cells or stably expressing BHK cell lines were grown at 37°C in an atmosphere of 5% CO_2 in Dulbecco's modified Eagle's medium (DMEM) supplemented with 10% (vol/vol) fetal bovine serum, 100 units/ml penicillin/streptomycin and 2 mM glutamine. 70-80% confluent cells grown in 35 mm dishes were split the day before transfection and transfected with 1 μg of wt or mutated Cx43-GFP cDNA and Superfect Transfection Reagent (Qiagen, Valencia, CA, USA) according to the manufacturer's instructions.

SDS-PAGE and immunoblot analysis

Complete cell lysates of transfected BHK cells were obtained by adding SDS-PAGE sample buffer to the cell monolayers. Samples were incubated for 30 minutes at room temperature (Cx32 expressing

cells) or boiled for 3 minutes (Cx43 expressing cells) and analyzed on 12.5% SDS-PAGE gels. Connexin proteins were characterized using rabbit antipeptide antibodies directed against the C-terminal tail of Cx43 (α1S) (Nishi et al., 1991) or a mouse monoclonal antibody generated against the C-terminal tail of Cx32 (β1S) (Falk et al., 1997), respectively, and secondary antibodies conjugated to horseradish peroxidase (Biorad, Hercules, CA). Blots were developed using the enhanced chemiluminescence system (Pierce, Rockford, IL). Relative expression levels were determined by comparing pixel intensities of each protein band by computer assisted analysis.

Immunofluorescence analysis

For immunolocalization, BHK cells were grown on coverslips placed into six well dishes and transfected with 1 μg of DNA. After 24 hours, cells were rinsed with phosphate-buffered saline (PBS), fixed in 4% (vol/vol) paraformaldehyde at room temperature for 15 minutes, permeabilized by placing them in 0.1% Triton X-100 in PBS for 90 seconds and stained with β1S antibodies followed by a secondary antibody conjugated to TRITC (tetra-methyl-rhodamine isothiocyanate) (Zymed, San Francisco, CA, USA). Cells were mounted using an antifade kit (Molecular Probes, Eugene, OR) and viewed with a Biorad 1024 confocal microscope or a Zeiss Axiovert 100 microscope with attached slide-film camera. GFP was detected by its green autofluorescence with an FITC filter set.

Dye transfer analysis

The ability of the various connexin variants to form functional gap junction channels was assayed by microinjecting a mixture of lucifer yellow [0.3% (wt/vol) in 0.1 M LiCl] and rhodamine B isothiocyanate-dextran (MW 40 kDa) [0.5% (wt/vol) in 0.1 M LiCl] (Sigma, St Louis, MO) into the cytoplasm of cells with visible connexin-GFP clusters assembled at cell-cell appositions. Transfer of lucifer yellow to coupled cells indicating functional gap junction channels was determined by imaging the cells 3 minutes after injection. Non-transfected BHK cells, and BHK cells transfected with wild-type Cx43-GFP were injected as controls. Representative cell monolayers before and after injection are shown in Fig. 3.

Statistical analysis

Fischer's exact test was used for statistical analysis of dye-transfer inhibition using GraphPad InStat software version 3.0a for Macintosh (GraphPad Software, San Diego, CA, USA, www.graphpad.com). Between 43 and 121 cells (functionally impaired variants), and 11 and 146 cells (controls) were injected to obtain significantly relevant ($P \leq 0.005$) results.

Results

Identification of amino-acid residues that discriminate between α and β connexins.

In order to elucidate amino-acid residues that are involved in regulating connexin interaction and assembly into connexons, we aligned human α and β type connexin amino-acid sequences and their mouse homologues (all human α subtypes and six β subtypes). The analysis was based on a systematic comparison of the physico-chemical properties (aliphatic, aromatic, polar, charge and size) of the amino-acid residues at each position. Interestingly, four positions were identified where the properties of the corresponding amino-acid residues of all analyzed α connexins were different from those of all analyzed β connexins. Two of these discriminatory residues (designated P1 and P2) were located in the cytoplasmic N-terminus (amino acids 12 and 13 of the α connexins, corresponding to amino acids 11 and 12 of β connexins) where the negatively charged residues aspartic acid (D) or glutamic acid (E), followed by the polar residues lysine (K), asparagine (N) or glutamine (Q) are present in α group connexins, whereas the small, non-charged residues serine (S) or glycine (G) are present in the β group connexins examined (Fig. 1A, Table 1). In addition, we identified two residues in the third transmembrane region TM3 (designated P3 and P4) at positions 152 and 153 of the Cx43 sequence (corresponding to various amino-acid residues in the other connexins owing to the variable length of the intracellular loops) where the non-aromatic residues leucine (L), methionine (M), arginine (R), glycine (G), or asparagine (N) were found in α group connexins, whereas the aromatic residue tryptophane (W) was invariably present in the β group connexins considered (Fig. 1A, Table 1). Other positions, where α connexins consistently differed from β connexins, were not found.

Assembly and function of Cx43 amino acid substitution variants

To test the hypothesis whether the identified amino-acid residues are involved in mediating connexin oligomerization compatibility, we constructed four single and one double GFP-tagged Cx43 variants, in which the characteristic Cx43 amino acid (an α group member) was substituted with the corresponding amino acid of Cx32 (a β group member) (designated D12S, K13G, DK12/13SG, L152W and R153W) and tested their ability to assemble into functional gap junctions (Fig. 1B, Table 1). BHK cells were transfected with the corresponding cDNAs, and successful expression of all Cx43 variants including their GFP-tags was observed by western blot analysis 24 hours post transfection (Fig. 2A, lanes 3-7, marked with an arrowhead). The level of wt Cx43-GFP expressed in parallel as a control was similar to the expression levels of the variants (Fig. 2A, lane 2). No Cx43-GFP protein was detected in non-transfected BHK cells (Fig. 2A, lane 1). A small amount of Cx43 endogenous to BHK cells was detected on over-exposed blots for all samples (Fig. 2A, lanes 1-7, marked with an asterisk). Additional bands detected correspond to phosphorylated Cx43-GFP (slower mobility), only partially denatured polypeptides, degradation products and/or unspecific immunoreaction products (faster mobility). To examine whether the Cx43 variants would assemble into gap junctions, variants were expressed in wt BHK cells. All Cx43-GFP variants appeared to assemble normally into connexons, gap junction channels and channel clusters as indicated by the appearance of large fluorescent connexin-GFP domains at cell-cell appositions (Fig. 2B). Furthermore, no difference in number and size of the clusters assembled from wt Cx43-GFP and Cx43 variants was observed (Fig. 2B), indicating that the single, and double amino-acid residue substitutions did not alter trafficking and assembly of the Cx43 variants. Similar results were observed in HEK 293 cells (data not shown).

To determine the function of channels assembled from Cx43 variants, transfected BHK cells with fluorescent connexin domains visible at cell-cell appositions were microinjected with a mixture of LY and rhodamine dextran (Fig. 3). Only the P4 variant R153W-GFP transferred LY at normal levels (100% dye transfer efficiency), indicating unaltered function (Fig. 3,

Fig. 4A). In all other Cx43 variants P1 (D12S-GFP), P2 (K13G-GFP), P1/2 (DK12/13SG-GFP), and P3 (L152W-GFP) LY dye coupling was reduced to background levels (5.2%, 8.1%, 2.8%, 3.2%) observed in untransfected BHK cells (6.9%), indicating that their function was impaired (Fig. 3, Fig. 4A). As expected, only LY (457 Da) was transferred between coupled cells, whereas rhodamine dextran (40 kDa) remained in the microinjected cells (Fig. 3, columns 3 and 4). Collectively, these results indicate that each of the residues present at positions 12 (aspartic acid), 13 (lysine) and 152 (leucine) plays a critical role for the normal function of Cx43 gap junction channels.

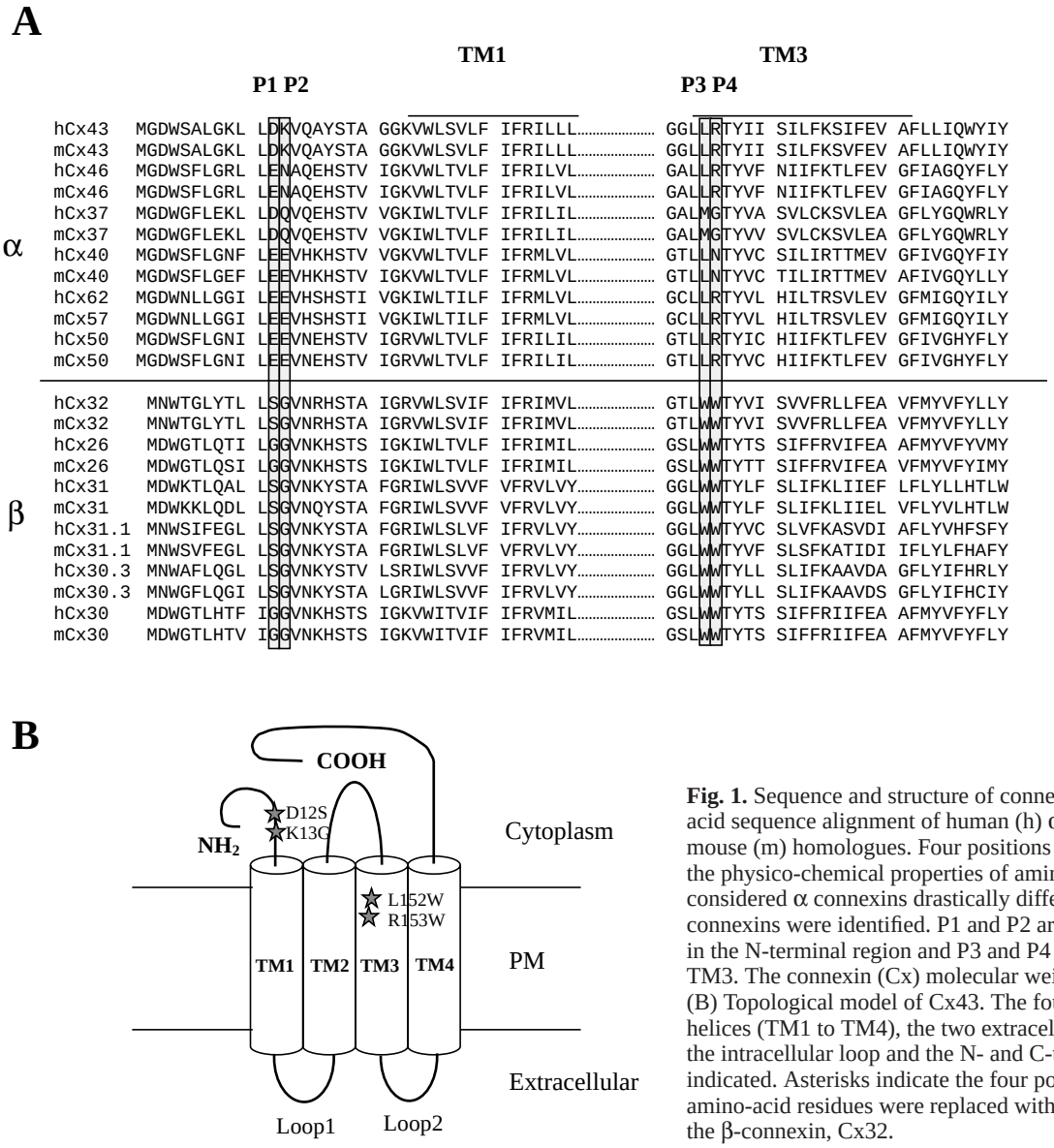

Fig. 1. Sequence and structure of connexin polypeptides. (A) Amino-acid sequence alignment of human (h) α and β connexins and their mouse (m) homologues. Four positions (P1 to P4, boxed) at which the physico-chemical properties of amino-acid residues in all considered α connexins drastically differed from all considered β connexins were identified. P1 and P2 are located next to each other in the N-terminal region and P3 and P4 at the cytoplasmic end of TM3. The connexin (Cx) molecular weight nomenclature was used. (B) Topological model of Cx43. The four trans-membrane spanning helices (TM1 to TM4), the two extracellular loops (Loop 1, Loop 2), the intracellular loop and the N- and C-terminal domains are indicated. Asterisks indicate the four positions where α-type specific amino-acid residues were replaced with corresponding residues of the β-connexin, Cx32.

Table 1. Amino acid properties of α and β connexins on discriminatory positions and corresponding Cx43 amino acid substitution variants*

Location†	α connexins	β connexins	Cx43 variant
P1 (12 in N-terminal tail)	Negatively charged D, E	Small, non-charged S, G	D12S
P2 (13 in N-terminal tail)	Polar K, N, Q, E	Small non-charged G	K13G DK12/13SG
P3 (152 in TM3)	Non-aromatic L, M	Aromatic W	L152W
P4 (153 in TM3)	Non-aromatic R, G, N	Aromatic W	R153W

*Physico-chemical properties of amino-acid residues discriminating α and β connexins at these positions are indicated. Amino-acid residues are given in single letter code.

†Amino acid positions correspond to the Cx43 sequence.

Dominant-negative inhibition of wt Cx43 by Cx43 variants

Assembly of LY-dye-transfer impaired channels by the Cx43 amino-acid exchange variants prompted us to investigate whether the non-functional variants exerted a dominant-negative effect on co-expressed wt Cx43 and disturbed its function. Thus, BHK cells stably transfected with Cx43 (BHK-Cx43) were transiently transfected with the cDNAs of the Cx43 amino-acid substitution variants, and levels of intercellular dye coupling were assessed. Experiments were carried out at two different Cx43 expression levels (approximately 2.5- and sixfold higher than endogenous Cx43 expression levels) in order to elucidate potential dose-dependent differences. Cx43 expression levels were modulated by the addition of different amounts of zinc acetate (Materials and Methods) (Kumar et al., 1995). At both Cx43 wt expression levels, the number of cells transferring dye was significantly (P<0.0001) higher (73.2% and 98.4%, Fig. 4B) than observed for non-transfected BHK cells (6.9%, Fig. 4A). Co-expression of Cx43 variants (P2) K13G, (P1/2) DK12/13SG and (P3) L152W resulted in a highly significant (P< 0.0001) decrease in dye coupling (to 24.0%, 22.6% and 32.0% at low Cx43 wt expression levels, and 64.7%, 49.0% and 43.1% at high Cx43 wt expression levels, Fig. 4A) consistent with a dominant inhibitory effect of these Cx43 variants on wt Cx43. The Cx43 variant (P1) D12S also exerted an inhibitory effect on co-expressed wt Cx43 (71.0% at low and 81.0% at high Cx43 wt expression levels, Fig. 4B); however, it was less pronounced (Fig. 4B). As expected, LY dye transfer by the functional Cx43 variant (P4) R153W was as efficient (100%) as in cells transfected with wt Cx43 (Fig. 4B). The more pronounced reduction of LY dye transfer capabilities at lower Cx43 wt expression levels demonstrates that the dominant negative inhibitory effect of the P1, P2 and P3 substitution variants was dose dependent (Fig. 4B).

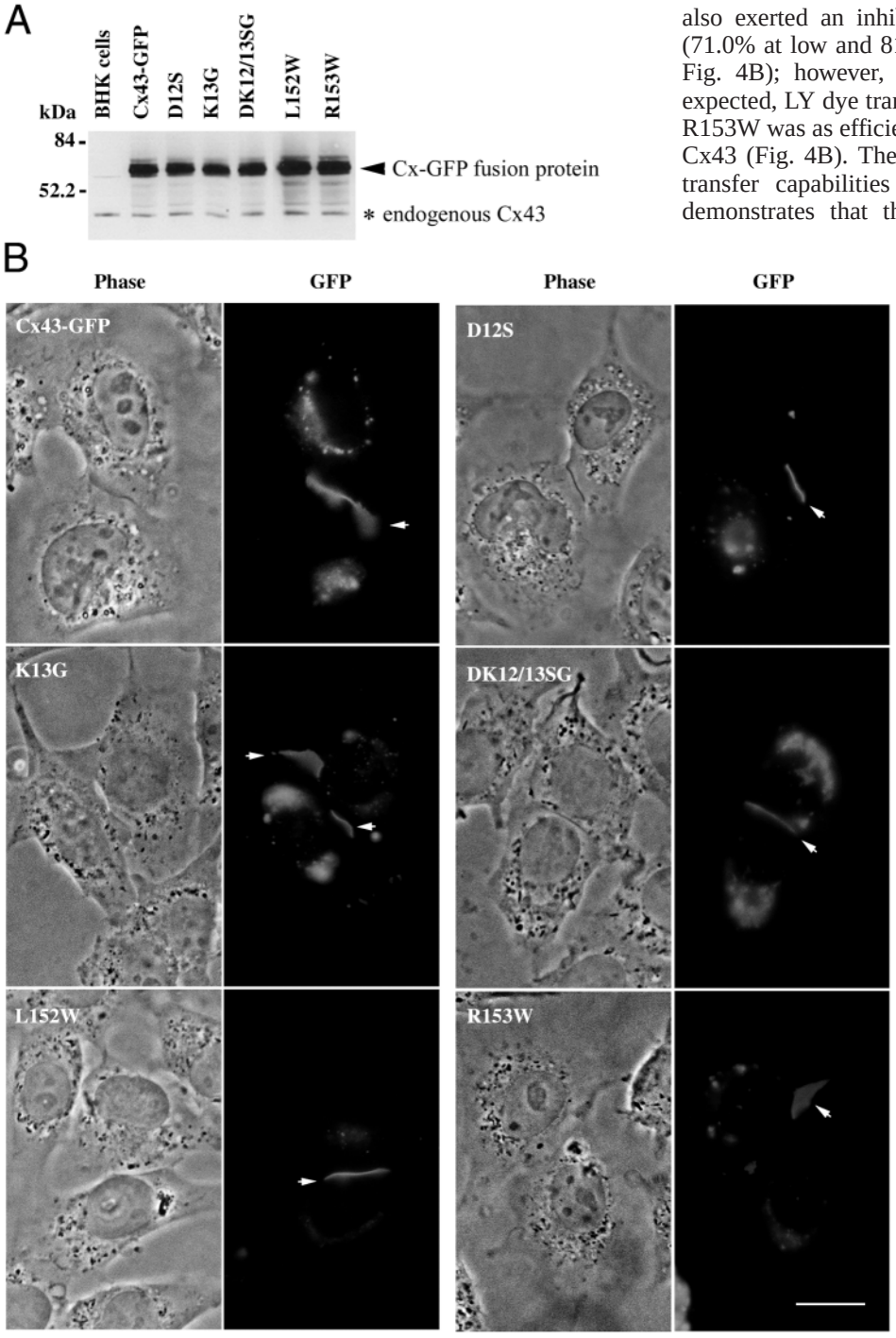

Trans-dominant-negative inhibition of wt Cx32 by Cx43 variants

To further examine whether the non-functional Cx43 variants might also have a trans-dominant negative effect on the function of Cx32 (a β-type connexin), similar co-expression experiments were performed in BHK cells that stably express wt Cx32 (BHK-Cx32) at lower

Fig. 2. Expression and localization of wildtype and Cx43 amino-acid substitution variants. (A) BHK cells were transfected with cDNAs encoding GFP-tagged wt and mutated Cx43, respectively, and expressed proteins were detected by western blot analysis using polyclonal antibodies directed against the C-terminal domain of Cx43. Equal amounts of full-length fusion proteins were expressed with all constructs (labeled with an arrowhead). Small amounts of endogenous Cx43 in BHK cells (labeled with an asterisk) and some unspecific reaction products were also detected in all lanes. (B) Localization of GFP-tagged connexins was detected by GFP auto-fluorescence 24 hours post transfection. Connexin clusters were detected with all constructs at cell-cell appositions (marked with arrows) besides intracellular fluorescence. Phase-contrast images are shown on the left; the corresponding fluorescence images are shown on the right. Bar, 10 μm.

(approximately 2.5-fold higher than endogenous Cx43) or higher (approximately fivefold over endogenous Cx43) levels. As expected, the percentage of cells transferring dye was significantly increased at both Cx32 expression levels (94.5% and 98.1%, $P<0.0001$, Fig. 4C) compared with untransfected BHK cells (6.9%, Fig. 4A). Co-expression of the Cx43 variants (P1) D12S, (P2) K13G and (P1/2) DK12/13SG in cells expressing lower levels of Cx32 also revealed a highly significant ($P<0.0001$) inhibition of co-expressed wt Cx32 channel function. Dye coupling was reduced to 58.6%, 45.3% and 53.3%, respectively (Fig. 4C). This trans-dominant inhibitory effect was also obvious in BHK cells expressing higher amounts of wt Cx32; however, again the effect was less pronounced (93.1%, 75.9% and 78.4%, Fig. 4C), also demonstrating the dose dependency of this trans-dominant inhibitory effect. In contrast, the Cx43 TM3 variant (P3) L152W reduced coupling only slightly (82.1% and 94.1%, respectively, Fig. 4C). The functional Cx43 variant (P4) R153W again had no detectable effect (100% coupling, Fig. 4C). Taken together, these results indicate that the N-terminal, but not the TM3 Cx43 variants, were able to inhibit the channel function of co-expressed Cx32.

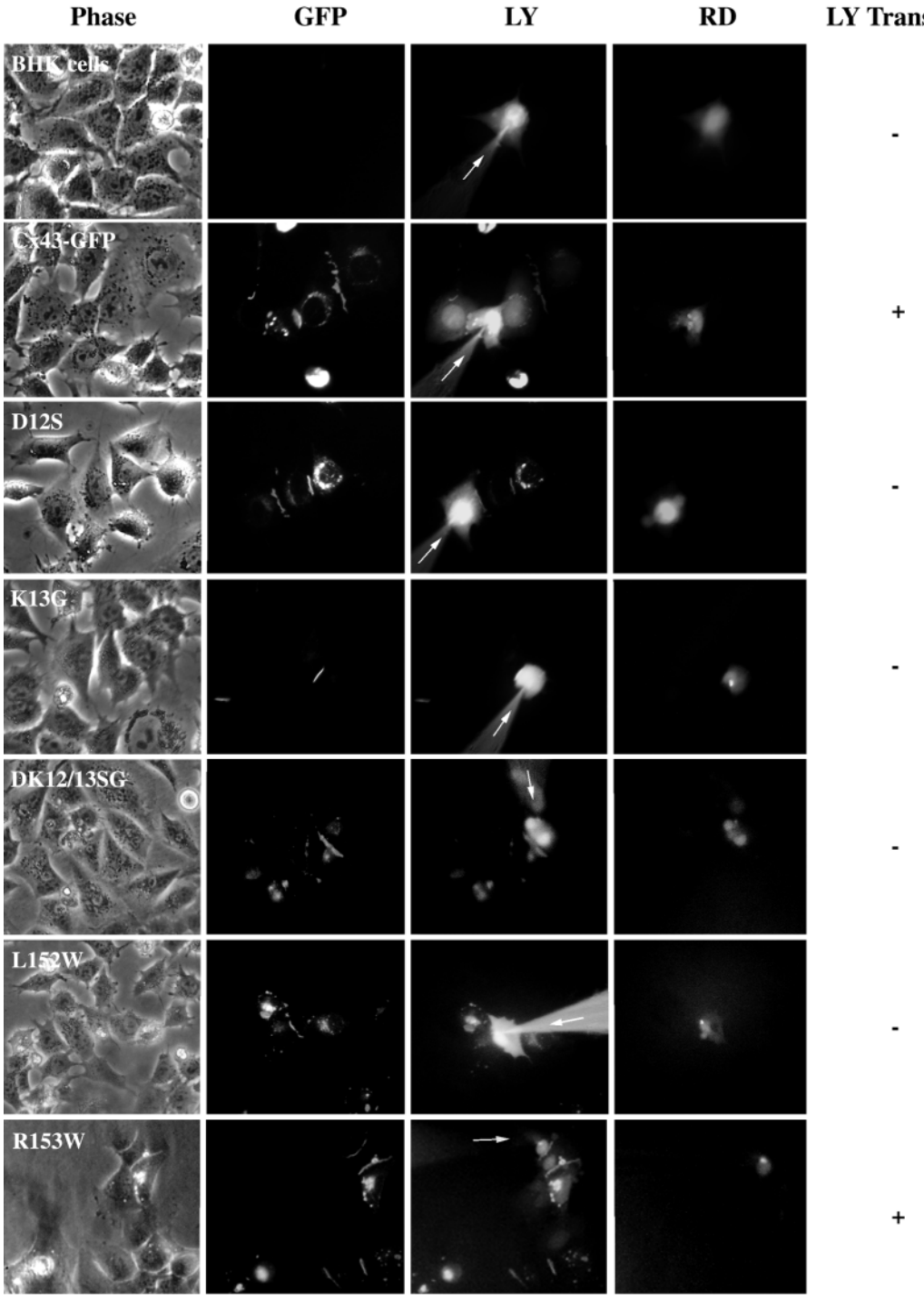

Fig. 3. Functional analysis of wildtype and Cx43 amino-acid substitution variants. Connexin-expressing BHK cells with assembled connexin clusters detectable by auto-fluorescence of their GFP-tags (GFP) were microinjected with a mixture of lucifer yellow (LY) and rhodamine dextran (RD), and their capacity to transfer LY to the neighboring cells was investigated. Although all Cx43 variants assembled into clusters, only Cx43 wt channels (row 2) and channels assembled from the R153W (P4) variant (row 7) transferred dye. BHK wild-type cells injected as controls (row 1) showed no dye coupling. Representative cells were imaged before and after microinjection (dye-filled injection capillaries visible on the LY images are marked with arrows). RD co-injected into the control did not pass to neighboring cells, indicating that cells were not leaking dye. Phase contrast images are shown on the left.

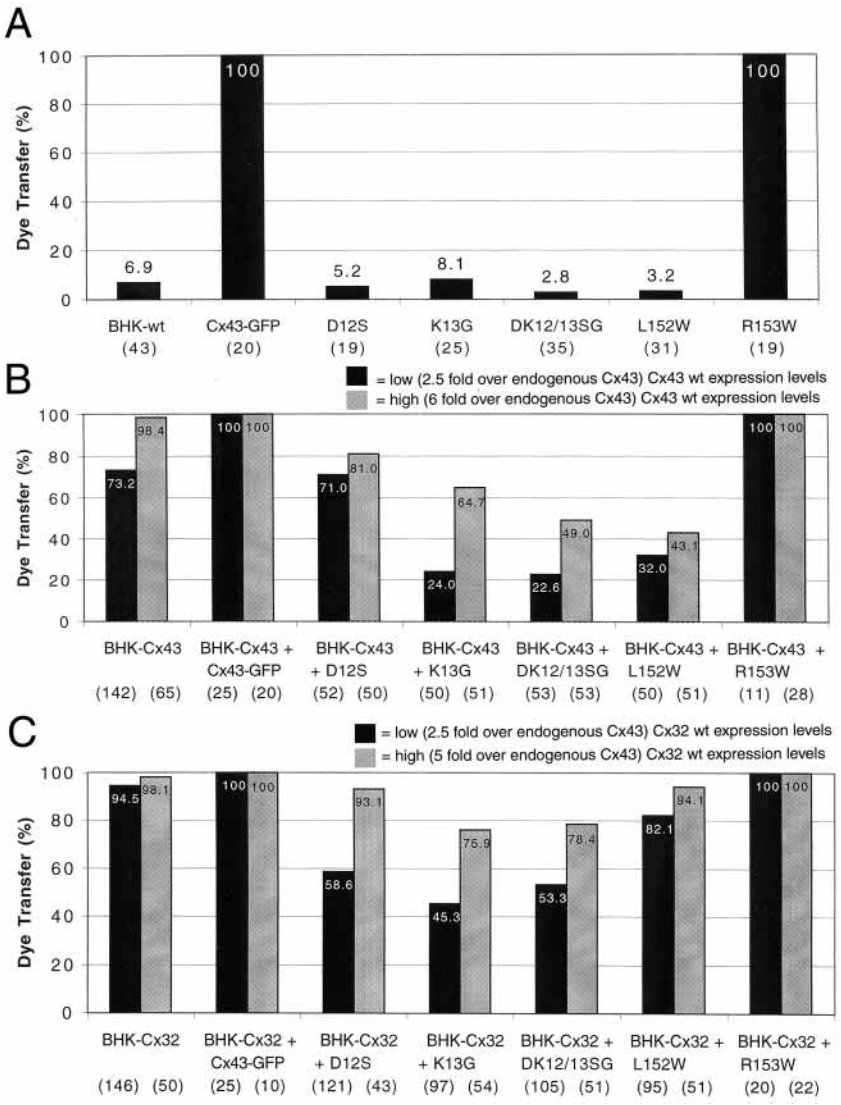

Fig. 4. Dye transfer efficiencies of Cx43 variants (A), dominant-negative (B) and trans-dominant-negative dye transfer inhibition (C) of co-expressed Cx43 and Cx32, respectively. Cells that transferred dye to neighboring cells were counted, and the percentage of cells transferring dye are shown as bars. Injections at low (black bars) and high (gray bars) wild-type Cx43 or wt Cx32 expression levels are shown in B and C. Total numbers of injected cells are given in parentheses under the names of the expressed proteins.

Colocalization of wt and Cx43 variants within connexin clusters

Dominant and trans-dominant inhibition of co-expressed Cx43 and Cx32 channel activity prompted us to explore whether the Cx43 variants would co-assemble with co-expressed wt connexins within the same junctional clusters. Cx43 variants were co-expressed in BHK cells stably transfected either with wt Cx43 (BHK-Cx43) or Cx32 (BHK-Cx32). After fixation, expressed Cx43 and Cx32 were labeled with specific monoclonal antibodies and visualized with a TRITC-coupled secondary antibody. Cx43 variants were visualized by using their GFP tag. In all instances, co-expressed wt connexin and the Cx43 variant assembled into connexin clusters that contained both connexin proteins, as shown by the yellow plaque color that resulted from merged red and green signals (shown for Cx32 wt and Cx43 variants in Fig. 5). In contrast, clusters assembled between cells expressing only wt Cx32 were red, whereas clusters between transfected cells that only expressed Cx43 variants were green (Fig. 5, marked with asterisks in the merged images of D12S and R152W).

Co-oligomerization of wt connexins and Cx43 variants into mixed connexons

To further analyze whether the dominant- and trans-dominant-negative inhibition of co-expressed wt Cx43 and Cx32 results from a direct interaction and oligomerization of variant and wt subunits into mixed connexons, we studied whether wt and variant connexin polypeptides interact. Thus, we co-expressed transport-deficient DsRed-tagged Cx43 or DsRed-tagged Cx32, respectively (Lauf et al., 2001), with the GFP-tagged substitution variants and assessed the interaction and assembly of the tagged proteins by the appearance of DsRed-tagged connexins within connexin clusters at cell-cell appositions (see Discussion). As expected, all Cx43 variants oligomerized with wt Cx43, as suggested by the presence of DsRed-tagged Cx43 in connexin clusters that were visible in the GFP, and the DsRed channels (Fig. 6A, rows 2-6, connexin clusters are labeled with arrows). Consistent with the less pronounced dominant inhibitory effect of the D12S variant described above, only a small amount of DsRed-tagged Cx43 was present in the clusters assembled by this variant (Fig. 6A, row 2). Wt Cx43 tagged with GFP and DsRed, respectively, co-expressed in control, also assembled into mixed connexons and gap junctions (Fig. 6A, row 1).

When GFP-tagged Cx43-variants were co-expressed with DsRed-tagged Cx32, only the N-terminal variants (D12S, K13G, and DK12/13SG), but not the TM3 variants (L152W, R153W) were able to rescue DsRed-tagged Cx32 that trafficked and co-assembled with the variants (Fig. 6B, rows 2-6, connexin clusters are labeled with arrows). This result is consistent with the trans-dominant inhibitory effect of the N-terminal Cx43 variants on co-expressed Cx32 described previously (Fig. 4C). As expected, wt Cx43-GFP co-expressed in control did not interact and rescue DsRed-tagged Cx32 (Fig. 6B, row 1).

Discussion

The present work was aimed at elucidating specific amino-acid residues that convey connexin oligomerization compatibility. By comparing α and β connexin sequences we identified four positions, an amino-acid doublet in the N-terminus (P1, P2), and a doublet in TM3 (P3, P4) where the physico-chemical

Table 2. Summary of Cx43 amino acid exchange variants

Variant	Connexin clusters*	Dye transfer	Co-oligomerization with co-expressed wt Cx43†	Inhibition of co-expressed Cx43 channel function	Co-oligomerization with co-expressed wt Cx32†	Inhibition of co-expressed Cx32 channel function
Cx43 wt	+	+	n.a.	n.a.	–	–
D12S	+	–	+‡	+‡	+	+
K13G	+	–	+	+	+	+
DK12/13SG	+	–	+	+	+	+
L152W	+	–	+	+	–	–
R153W	+	+	+	–	–	–

*Based on fluorescence light microscopic inspection and dye transfer ability.
†Based on colocalization and rescue of transport deficient Cx43-DsRed, or Cx-32-DsRed, respectively.
‡Weak affinity and inhibitory effect.
n.a., not applicable.

properties of corresponding amino-acid residues differ consistently between α and β connexins (Fig. 1, Table 1). A similar alignment strategy has been used previously with aquaporin water-channel subunit proteins that led to the identification of five discriminatory residues (Froger et al., 1998). Substitution of two of these residues altered the channel preference and transformed the water channel into a glycerol channel (Lagree et al., 1999). Replacement of three of the identified residues in Cx43 (P1, P2 and P3) with orthologous β-type specific residues from Cx32 (Fig. 1, Table 1) resulted in a functional impairment of the variants (indicated by their lost ability to transfer LY; Fig. 3, 4A), despite assembly of all of the variants into gap junctions (suggested by their fluorescence light microscopic appearance; Fig. 2). Previously, oligomerization into hexameric connexons has been shown to be a necessary prerequisite for trafficking and assembly of gap junctions at cell-cell appositions (Musil and Goodenough, 1993). Thus, all Cx43 substitution variants must have been oligomerized into connexons. Functional inhibition did not simply result from tagging Cx43 and variants with GFP. GFP-tagged wt Cx43, consistent with previous results (Bukauskas et al., 2000; Falk, 2000; Jordan et al., 1999), as well as the GFP-tagged P4 variant, exerted unaltered LY dye coupling capabilities (Fig. 4A). Interestingly, mutations at both positions in the N-terminus and TM3 that we have identified have also been found in connexins of patients that suffer from connexin-related diseases. Missense, nonsense and frame-shift mutations have been identified at these positions (reviewed in Yum et al., 2002) that result in the generation of transport deficient [e.g. D12S (P2) in Cx32] (Deschenes et al., 1997) or functionally impaired channels [e.g. G12R, and G12D (P2) in Cx31, W133C (P4) in Cx32] (Diestel et al., 2002; Rouan et al., 2003; Skerrett et al., 2002).

Location of the identified amino acids

Relatively little is known about the role of the N-terminal domain in the function of connexins. Some evidence suggests that the N-terminal tail is part of the voltage sensor and plays a fundamental role in ion permeation. Residues 1-10 of β-connexins are predicted to lie within the channel pore, and the N-terminal domain might form the channel vestibule (Purnick et al., 2000). The substitutions at P1 and P2 of Cx43 described here reduce the net charge of this domain and, thus, might cause the functional impairment of these substitution variants. On the other hand, recent experiments by Purnick et al. suggest that G12 in Cx32 (P2) create a turn in the N-terminal tail that is necessary for the function of this connexin (Purnick et al., 2000). Substitution of the Cx32 G12 residue with amino acids expected to reduce the flexibility of this domain (such as serine, valine and tyrosine) abolished junctional currents. However, when G12 was substituted with proline, which is often found in turns and expected to maintain flexibility, the expressed Cx32 G12P variant formed functional channels. These findings were further corroborated by structural analyses of a synthetic peptide of this region that folded into two α helices connected by a flexible hinge (Purnick et al., 2000). Since no glycine or proline is present at, or close to, the P1/P2 position of α-connexins, the structural conformation of their N-terminal domain is likely to differ from that of β connexins. Thus, it is tempting to speculate whether our experimental introduction of glycine into the N-terminal tail of Cx43, by analogy, may have created a turn in this domain and therefore rendered channels composed of these Cx43 variants non-functional (see below).

The third trans-membrane-spanning domain (TM3) has been hypothesized to line the aqueous pore of gap junction channels (Milks et al., 1988). This has been confirmed recently by systematic cysteine mutagenesis of Cx32 (Skerrett et al., 2002). Leucine (L) to tryptophan (W) exchange at position 152 (P3) located at the cytoplasmic end of TM3 resulted in a LY-dye-transfer-impaired, but apparently normally assembling, gap junction channel, similar to that observed for the P1 and P2 variants. Exchanging the corresponding amino-acid residue in Cx32 (tryptophan) with the corresponding amino-acid residue of Cx43 (leucine) also resulted in an impaired extremely short-lived connexin (data not shown). However, exchange of the directly adjacent arginine 153 (P4) with the homologue Cx32 residue (also tryptophan) (R153W) did not result in any detectable negative effect on Cx43, whereas the corresponding Cx32 variant (W133R) is a naturally occurring Cx32 CMTX mutation (Bone et al., 1995), and changing tryptophan 133 in Cx32 into cysteine (W133C) results in non-functional channels (Skerrett et al., 2002). Results comparable to ours observed for the non-functional Cx43 variants (P1-P3) were recently reported (e.g. Skerrett et al., 2002; Oshima et al., 2003), who found that three of the 48 cysteine mutations in Cx32 (W77C, W133C and T134C) and mutation of methionine 34 into alanine (M34A) in Cx26 resulted in fully assembled but non-functional channels.

Interestingly, as mentioned above, W133 in Cx32 is homologous to R153 in Cx43 that we have identified as critical

position P4. It is believed that such critical residues that interfere with function but allow channel assembly are located at strategic positions, where they define the position of the trans-membrane helices (Skerrett et al., 2002) or interact with adjacent connexin subunits within the connexon to ensure an open channel structure (Oshima et al., 2003).

Dominant and trans-dominant inhibition by Cx43 substitution variants

All non-functional Cx43 substitution variants (P1-P3) exerted a dominant-negative effect on the dye-coupling of co-expressed wt Cx43 channels (Fig. 4B). The N-terminal variants (P1, P2) exerted, in addition, a trans-dominant-negative inhibitory effect on the dye-coupling of co-expressed Cx32 (a β-connexin) channels (summarized in Table 2). A similar dominant and trans-dominant-negative effect has been reported for naturally occurring, disease-causing connexin mutations. For example, mutations of the β-connexin Cx26, ΔE42, W44C, D66H and R75W have been found to inhibit co-expressed wt Cx26 function (Oshima et al., 2003; Richard et al., 1998; Rouan et al., 2001). In addition, all these mutants except W44C were found to also inhibit the channel function of the co-expressed α-connexin Cx43 (Rouan et al., 2001). Dominant and trans-dominant inhibition might be explained by the interaction of wt and variant connexin subunits that co-oligomerize into mixed connexons and thus render the resulting mixed connexons and gap junction channels non-functional.

Evidence for direct interaction and co-oligomerization of wt and variant connexin subunits was obtained in our study. Previously, we have demonstrated that DsRed-tagged connexins are transport-deficient and will not assemble into gap junction plaques in the plasma membrane (Lauf

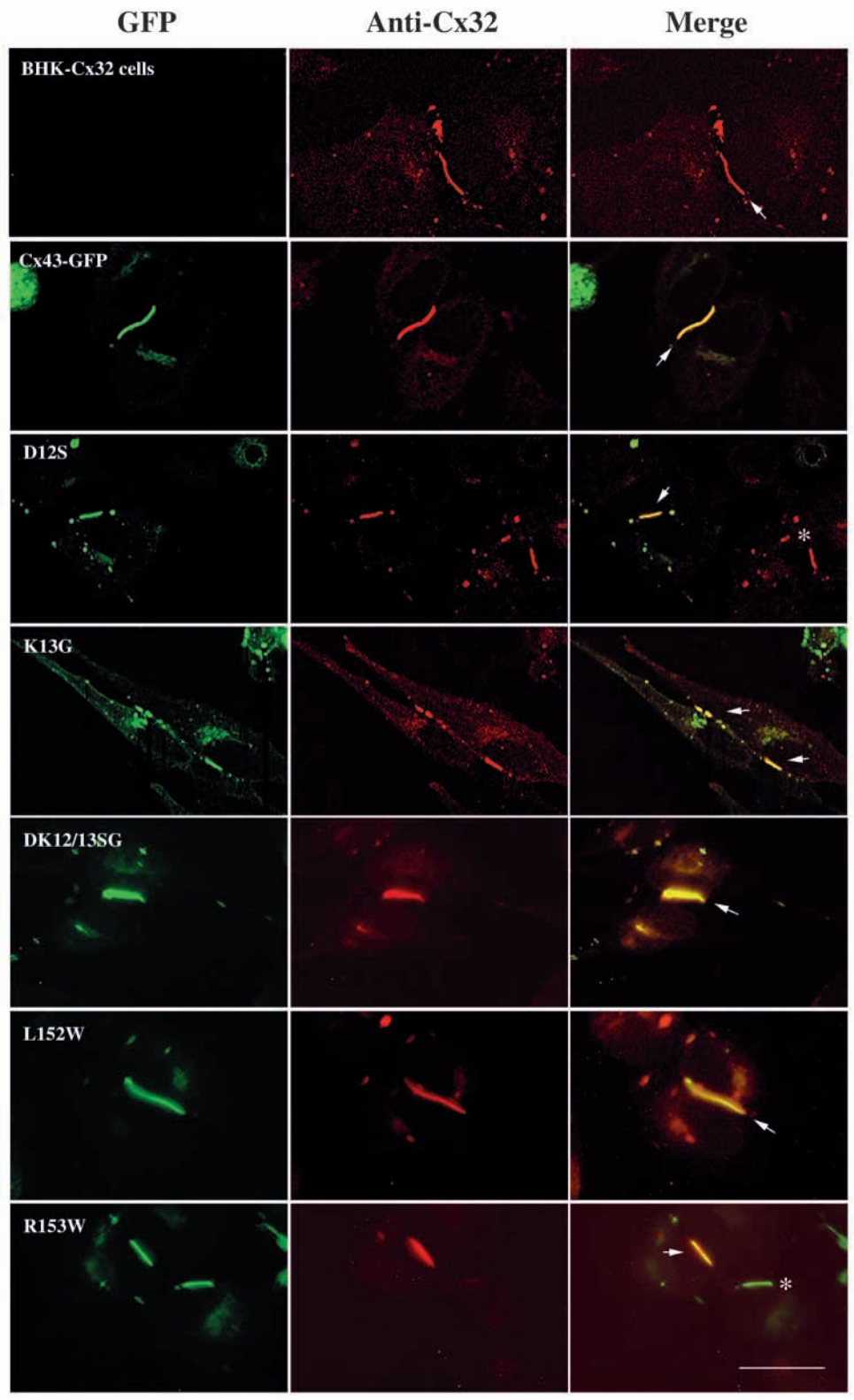

Fig. 5. Cx43 amino-acid substitution variants and Cx32 colocalize within connexin clusters at cell-cell appositions. Stably transfected BHK cells expressing Cx32 (BHK-Cx32) were co-transfected with wildtype or Cx43-GFP substitution variants, respectively. In all instances, both connexin isotypes localized to the same connexin clusters (labeled with arrows) as indicated by the yellow plaque color in the merged images (Merge). Cx32 was immunostained with Cx32-specific antibodies followed by TRITC-coupled secondary antibodies 24 hours after transfection and fixation (Anti-Cx32, red). Wild-type Cx43 and variants were detected by their GFP auto-fluorescence (GFP, green). Connexin clusters assembled between cells that expressed only Cx43 appeared green, clusters in cells that expressed only Cx32 appeared red (labeled with asterisks in the merged images of variants D12S, and R153W). Bar, 20 μm.

et al., 2001). However, co-expression of wt or GFP-tagged connexin-polypeptides together with transport-deficient DsRed-tagged connexins will recover trafficking of DsRed-tagged connexin polypeptides that then localize within connexin clusters at cell-cell appositions. Successful trafficking of DsRed-tagged connexins appears to result from the co-oligomerization of untagged or GFP-tagged connexin subunits with DsRed-tagged connexins into mixed connexons (Lauf et al., 2001). Comparable approaches that either deployed transport-deficient connexins tagged with β-galactosidase, or connexins tagged with endoplasmic reticulum retention signals have also been developed recently and have been used to investigate intracellular interaction and co-assembly of co-expressed connexin isoforms (Das Sarma et al., 2001; Das Sarma et al., 2002). Consistent with the dominant-negative effect, P1, P2 and P3 Cx43 variants were able to recover trafficking of co-expressed DsRed-tagged wt Cx43 as indicated by its colocalization with GFP-tagged variant subunits in connexin clusters at cell-cell appositions (Fig. 6A). In addition, the N-terminal, but not the TM3, variants were able to recover trafficking of co-expressed DsRed-tagged Cx32 (Fig. 6B), consistent with their ability to inhibit dye transfer of co-expressed Cx32 channels (Fig. 4C). Co-assembly of wt and variant connexin subunits into functionally impaired, mixed connexons is further supported by the assembly of connexins into connexons that is a prerequisite for trafficking and channel formation (Musil and Goodenough, 1993) and the dose-dependent dominant and trans-dominant inhibitory effects that were proportional to the amount of co-expressed wt connexins (Fig. 4B,C).

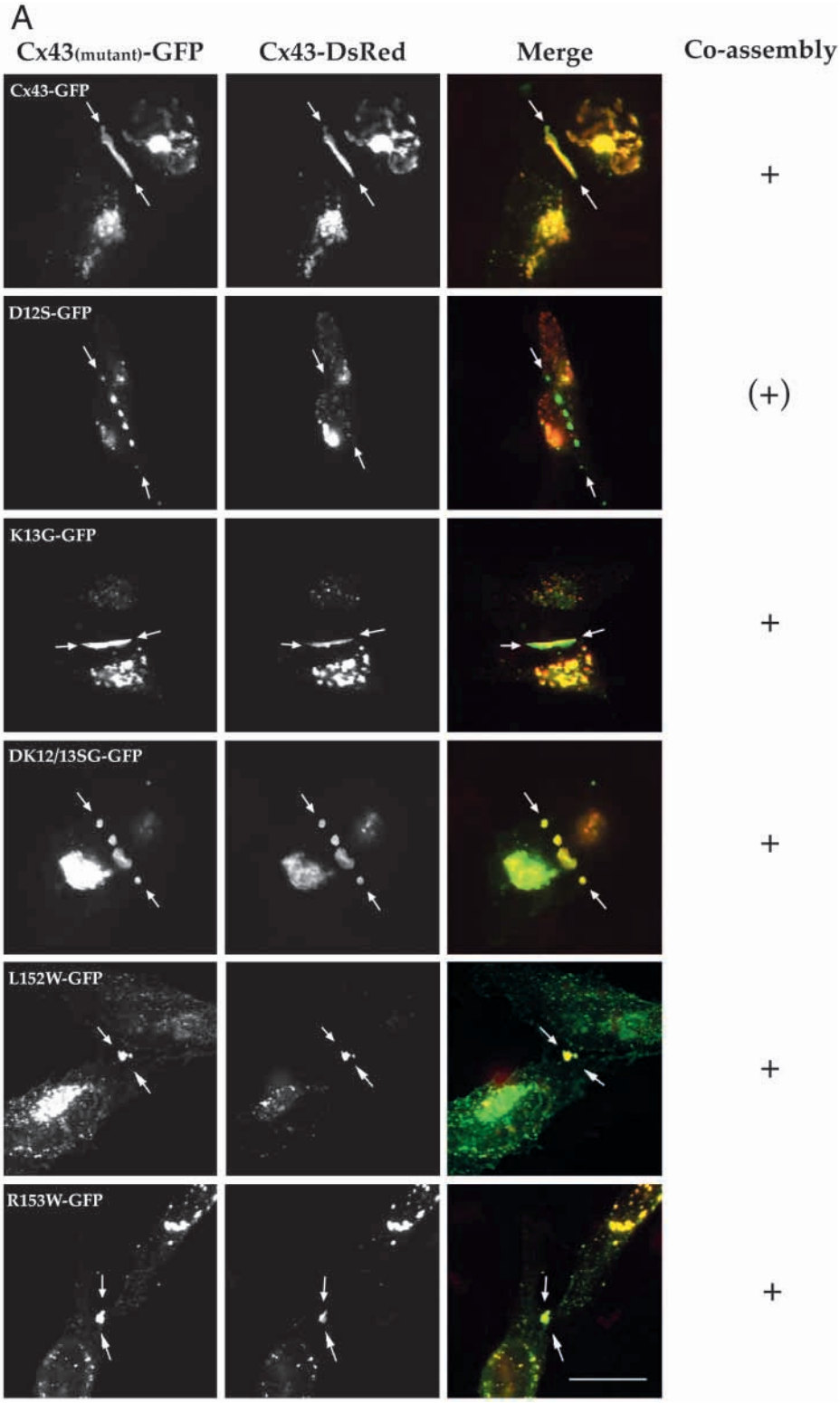

By co-expressing full-length connexins together with N-terminally truncated variants in cell-free translation/membrane translocation assays, we had previously obtained evidence that a distinct amino-acid signal is located in the N-terminal portion of the connexin sequence (N-terminal domain, TM1, and/or first extra-cellular loop) that is involved in regulating recognition and assembly compatibility of α (Cx43) and β (Cx26, Cx32) connexins (Falk et al., 1997). On the basis of our previous and current results we speculate that connexin polypeptide recognition and oligomerization compatibility depend on different structural motifs that include amino-acid residues at positions P1 and P2. These structural differences might allow connexins with similarly folded motifs to interact and oligomerize but prevents the interaction and oligomerization of connexin polypeptides with differently folded motifs. Such structural motifs have been found previously in the N-terminal region of other membrane channels, such as acetylcholine receptors, potassium channels,

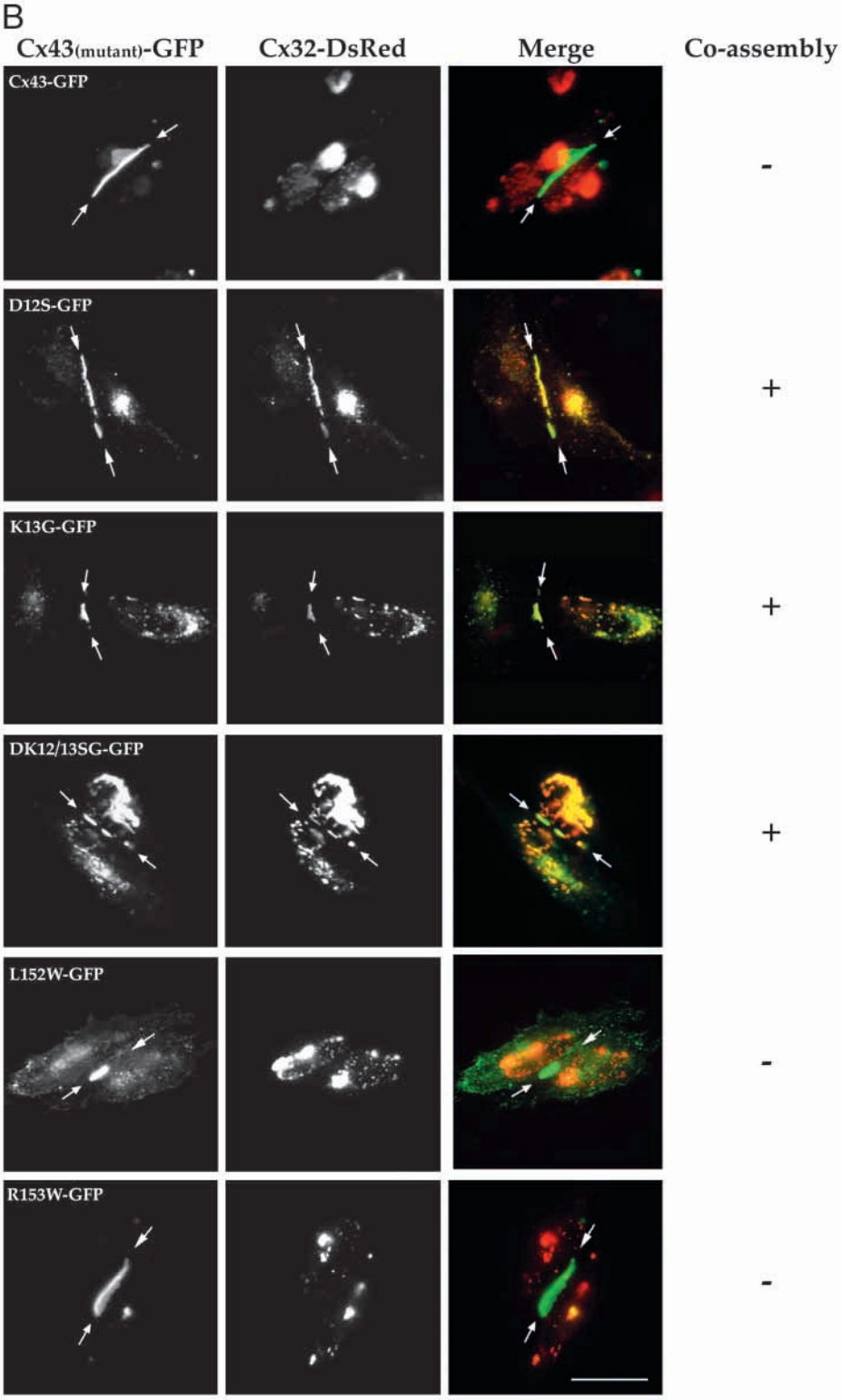

Fig. 6. Assessment of wildtype and Cx43 variant interaction and co-oligomerization. Transport-deficient DsRed-tagged Cx43 (A) or Cx32 (B) were co-expressed with GFP-tagged Cx43 variants. Interaction and co-assembly of DsRed-tagged wildtype and GFP-tagged variant connexin subunits into mixed connexons were evident by the successful trafficking of DsRed-tagged connexin subunits to the plasma membrane and their localization together with GFP-tagged connexins in connexin clusters that were detectable in the GFP and the DsRed channels (clusters are labeled with arrows). Clusters in merged images appear more or less yellow dependent on the ratios of GFP and DsRed-tagged subunits. Cx43 wildtype was co-expressed in control (rows 1 in A and B). Bar, 20 μm.

GlyR receptors, and $GABA_A$ receptors (Griffon et al., 1999; Li et al., 1992; Shen et al., 1993; Taylor et al., 1999; Verrall and Hall, 1992). However, since additional amino-acid residue mutations located downstream in the first extracellular domain (E42, W44, D66 and R75) were also found to be involved in a trans-dominant inhibition of Cx26 variants, different signals, different structural motifs or, more likely, compound structural motifs, which consist of different segments of the connexin polypeptides, regulate recognition and co-oligomerization of connexin isoforms.

Dominant and trans-dominant inhibition and connexin disorders

In both the inner ear and epidermis a number of β-connexins (such as Cx26, Cx30, Cx30.3, Cx31, Cx31.1 and Cx32) are expressed in overlapping, spatial and temporal patterns with α-connexins (such as Cx37 and Cx43) (Liu et al., 2001; Rouan et al., 2001). Mutations in most of these connexins underlie distinct genetic forms of deafness and skin disorders (Liu et al., 2001; Rouan et al., 2001). Interestingly, several missense mutations have recently been identified in three different β-connexin genes that also affect positions P1 and P2 (e.g. G11R (P1) in Cx30 (Lamartine et al., 2000), G12R (P2) in Cx26 (Richard et al., 2002) and G12D and G12R (P2) in Cx31 (Richard et al., 1998). Functional analyses of the Cx31 mutants in mammalian expression systems revealed that both Cx31 mutations did not obviously interfere with expression, connexon assembly and targeting to the cell membrane, but significantly altered channel function (Diestel et al., 2002; Rouan et al., 2003). On the basis of the trans-dominant inhibitory effect of the Cx43 P1 and P2 amino acid exchange variants described in this study and the trans-dominant Cx26 variants described above (Rouan et al., 2001), it appears possible that an aberrant hetero-oligomerization between co-expressed mutant and wt α and β-connexins cause disease phenotypes in certain cases of connexin-related disorders. Further experiments will elucidate

connexin subunit oligomerization under normal and pathological conditions.

We thank Malcolm Wood and the Scripps Microscopy Core Facility for initial assistance with confocal microscopy, and Nalin Kumar and members of the Gilula laboratory for critical suggestions and technical assistance. This work was supported by NIH grants GM37904 to N.B.G., K08-AR02141 to G.R., and GM55725 to M.M.F.

References

Bennett, M. V., Zheng, X. and Sogin, M. L. (1994). The connexins and their family tree. *Soc. Gen. Physiol. Series* **49**, 223-233.

Berthoud, V. M., Montegna, E. A., Atal, N., Aithal, N. H., Brink, P. R. and Beyer, E. C. (2001). Heteromeric connexons formed by the lens connexins, connexin43 and connexin56. *Eur. J. Cell Biol.* **80**, 11-19.

Bevans, C. G., Kordel, M., Rhee, S. K. and Harris, A. L. (1998). Isoform composition of connexin channels determines selectivity among second messengers and uncharged molecules. *J. Biol. Chem.* **273**, 2808-2816.

Bone, L. J., Dahl, N., Lensch, M. W., Chance, P. F., Kelly, T., le Guern, E., Magi, S., Parry, G., Shapiro, H. and Wang, S. (1995). New connexin32 mutations associated with X-linked Charcot-Marie-Tooth disease. *Neurology* **45**, 1863-1866.

Brink, P. R., Cronin, K., Banach, K., Peterson, E., Westphale, E. M., Seul, K. H., Ramanan, S. V. and Beyer, E. C. (1997). Evidence for heteromeric gap junction channels formed from rat connexin43 and human connexin37. *Am. J. Physiol.* **273**, C1386-C1396.

Bruzzone, R., White, T. W. and Goodenough, D. A. (1996). The cellular Internet: on-line with connexins. *Bioessays* **18**, 709-718.

Bukauskas, F. F., Jordan, K., Bukauskiene, A., Bennett, M. V., Lampe, P. D., Laird, D. W. and Verselis, V. K. (2000). Clustering of connexin 43-enhanced green fluorescent protein gap junction channels and functional coupling in living cells. *Proc. Natl. Acad. Sci. USA* **97**, 2556-2561.

Cottrell, G. T. and Burt, J. M. (2001). Heterotypic gap junction channel formation between heteromeric and homomeric Cx40 and Cx43 connexons. *Am. J. Physiol. Cell Physiol.* **281**, C1559-C1567.

Dahl, G., Werner, R., Levine, E. and Rabadan-Diehl, C. (1992). Mutational analysis of gap junction formation. *Biophys. J.* **62**, 172-182.

Das Sarma, J., Meyer, R. A., Wang, F., Abraham, V., Lo, C. W. and Koval, M. (2001). Multimeric connexin interactions prior to the trans-Golgi network. *J. Cell Sci.* **114**, 4013-4024.

Das Sarma, J. D., Wang, F. and Koval, M. (2002). Targeted gap junction protein constructs reveal connexin-specific differences in oligomerization. *J. Biol. Chem.* **277**, 20911-20918.

Deschenes, S. M., Walcott, J. L., Wexler, T. L., Scherer, S. S. and Fischbeck, K. H. (1997). Altered trafficking of mutant connexin32. *J. Neuroscience* **17**, 9077-9084.

Diestel, S., Richard, G., Doring, B. and Traub, O. (2002). Expression of a connexin31 mutation causing erythrokeratodermia variabilis is lethal for HeLa cells. *Biochem. Biophys. Res. Commun.* **296**, 721-728.

Falk, M. M. (2000). Biosynthesis and structural composition of gap junction intercellular membrane channels. *Eur. J. Cell Biol.* **79**, 564-574.

Falk, M. M. and Gilula, N. B. (1998). Connexin membrane protein biosynthesis is influenced by polypeptide positioning within the translocon and signal peptidase access. *J. Biol. Chem.* **273**, 7856-7864.

Falk, M. M., Kumar, N. M. and Gilula, N. B. (1994). Membrane insertion of gap junction connexins: polytopic channel forming membrane proteins. *J. Cell Biol.* **127**, 343-355.

Falk, M. M., Buehler, L. K., Kumar, N. M. and Gilula, N. B. (1997). Cell-free synthesis and assembly of connexins into functional gap junction membrane channels. *EMBO J.* **16**, 2703-2716.

Froger, A., Tallur, B., Thomas, D. and Delamarche, C. (1998). Prediction of functional residues in water channels and related proteins. *Protein Sci.* **7**, 1458-1468.

Goldberg, G. S., Lampe, P. D. and Nicholson, B. J. (1999). Selective transfer of endogenous metabolites through gap junctions composed of different connexins. *Nat. Cell Biol.* **1**, 457-459.

Goodenough, D. A., Goliger, J. A. and Paul, D. L. (1996). Connexins, connexons, and intercellular communication. *Annu. Rev. Biochem.* **65**, 475-502.

Green, W. N. and Millar, N. S. (1995). Ion-channel assembly. *Trends Neurosci.* **18**, 280-287.

Griffon, N., Buttner, C., Nicke, A., Kuhse, J., Schmalzing, G. and Betz, H. (1999). Molecular determinants of glycine receptor subunit assembly. *EMBO J.* **18**, 4711-4721.

He, D. S., Jiang, J. X., Taffet, S. M. and Burt, J. M. (1999). Formation of heteromeric gap junction channels by connexins 40 and 43 in vascular smooth muscle cells. *Proc. Natl. Acad. Sci. USA* **96**, 6495-6500.

Hertzberg, E. L., Disher, R. M., Tiller, A. A., Zhou, Y. and Cook, R. G. (1988). Topology of the Mr 27,000 liver gap junction protein. Cytoplasmic localization of amino- and carboxyl termini and a hydrophilic domain which is protease-hypersensitive. *J. Biol. Chem.* **263**, 19105-19111.

Jiang, J. X. and Goodenough, D. A. (1996). Heteromeric connexons in lens gap junction channels. *Proc. Natl. Acad. Sci. USA* **93**, 1287-1291.

Jordan, K., Solan, J. L., Dominguez, M., Sia, M., Hand, A., Lampe, P. D. and Laird, D. W. (1999). Trafficking, assembly, and function of a connexin43-green fluorescent protein chimera in live mammalian cells. *Mol. Biol. Cell* **10**, 2033-2050.

Kelsell, D. P., Dunlop, J. and Hodgins, M. B. (2001). Human diseases: clues to cracking the connexin code? *Trends Cell Biol.* **11**, 2-6.

Konig, N. and Zampighi, G. A. (1995). Purification of bovine lens cell-to-cell channels composed of connexin44 and connexin50. *J. Cell Sci.* **108**, 3091-3098.

Kumar, N. M., Friend, D. S. and Gilula, N. B. (1995). Synthesis and assembly of human beta 1 gap junctions in BHK cells by DNA transfection with the human beta 1 cDNA. *J. Cell Sci.* **108**, 3725-3734.

Kumar, N. M. and Gilula, N. B. (1992). Molecular biology and genetics of gap junction channels. *Semin. Cell Biol.* **3**, 3-16.

Kumar, N. M. and Gilula, N. B. (1996). The gap junction communication channel. *Cell* **84**, 381-388.

Lagree, V., Froger, A., Deschamps, S., Hubert, J. F., Delamarche, C., Bonnec, G., Thomas, D., Gouranton, J. and Pellerin, I. (1999). Switch from an aquaporin to a glycerol channel by two amino acids substitution. *J. Biol. Chem.* **274**, 6817-6819.

Lamartine, J., Munhoz Essenfelder, G., Kibar, Z., Lanneluc, I., Callouet, E., Laoudj, D., Lemaitre, G., Hand, C., Hayflick, S. J., Zonana, J. et al. (2000). Mutations in GJB6 cause hidrotic ectodermal dysplasia. *Nat. Genet.* **26**, 142-144.

Lauf, U., Lopez, P. and Falk, M. M. (2001). Expression of fluorescently tagged connexins: a novel approach to rescue function of oligomeric DsRed-tagged proteins. *FEBS Lett.* **498**, 11-15.

Li, M., Jan, Y. N. and Jan, L. Y. (1992). Specification of subunit assembly by the hydrophilic amino-terminal domain of the Shaker potassium channel. *Science* **257**, 1225-1230.

Liu, X. Z., Xia, X. J., Adams, J., Chen, Z. Y., Welch, K. O., Tekin, M., Ouyang, X. M., Kristiansen, A., Pandya, A., Balkany, T. et al. (2001). Mutations in GJA1 (connexin 43) are associated with non-syndromic autosomal recessive deafness. *Hum. Mol. Genet.* **10**, 2945-2951.

Locke, D., Perusinghe, N., Newman, T., Jayatilake, H., Evans, W. H. and Monaghan, P. (2000). Developmental expression and assembly of connexins into homomeric and heteromeric gap junction hemichannels in the mouse mammary gland. *J. Cell. Physiol.* **183**, 228-237.

Milks, L. C., Kumar, N. M., Houghten, R., Unwin, N. and Gilula, N. B. (1988). Topology of the 32-kd liver gap junction protein determined by site-directed antibody localizations. *EMBO J.* **7**, 2967-2975.

Musil, L. S. and Goodenough, D. A. (1993). Multisubunit assembly of an integral plasma membrane channel protein, gap junction connexin43, occurs after exit from the ER. *Cell* **74**, 1065-1077.

Nishi, M., Kumar, N. M. and Gilula, N. B. (1991). Developmental regulation of gap junction gene expression during mouse embryonic development. *Dev. Biol.* **146**, 117-130.

Oshima, A., Doi, T., Mitsuoka, K., Maeda, S. and Fujiyoshi, Y. (2003). Roles of M34, C64, and R75 in the assembly of human connexin 26: Implication for key amino acid residues for channel formation and function. *J. Biol. Chem.* **278**, 1807-1816.

Purnick, P. E., Benjamin, D. C., Verselis, V. K., Bargiello, T. A. and Dowd, T. L. (2000). Structure of the amino terminus of a gap junction protein. *Archives Biochem. Biophys.* **381**, 181-190.

Richard, G. (2001). Connexin disorders of the skin. *Adv. Dermatol.* **17**, 243-277.

Richard, G., Smith, L. E., Bailey, R. A., Itin, P., Hohl, D., Epstein, E. H., Jr, DiGiovanna, J. J., Compton, J. G. and Bale, S. J. (1998). Mutations in the human connexin gene GJB3 cause erythrokeratodermia variabilis. *Nat. Genet.* **20**, 366-369.

Richard, G., Rouan, F., Willoughby, C. E., Brown, N., Chung, P., Ryynänen, M., Jabs, E. B., Bale, S. J., DiGiovanna, J. J., Uitto, J. et al.

(2002). Missense mutations in GJB2 encoding connexin-26 cause the ectodermal dysplasia Keratitis-Ichthyosis-Deafness syndrome. *Am. J. Hum. Genet.* **70**, 1341-1348.

Rouan, F., Lo, C., Fertala, A., Wahl, M., Rodeck, U., Uitto, J. and Richard, G. (2003). Divergent effects of two sequence variants of GJB3 (G12D and R32W) on the function of connexin 31 in vitro. *Exp. Dermatol.* **12**, 191-197.

Rouan, F., White, T. W., Brown, N., Taylor, A. M., Lucke, T. W., Paul, D. L., Munro, C. S., Uitto, J., Hodgins, M. B. and Richard, G. (2001). Trans-dominant inhibition of connexin-43 by mutant connexin-26: implications for dominant connexin disorders affecting epidermal differentiation. *J. Cell Sci.* **114**, 2105-2113.

Rubin, J. B., Verselis, V. K., Bennett, M. V. and Bargiello, T. A. (1992). Molecular analysis of voltage dependence of heterotypic gap junctions formed by connexins 26 and 32. *Biophys. J.* **62**, 183-195.

Shen, N. V., Chen, X., Boyer, M. M. and Pfaffinger, P. J. (1993). Deletion analysis of K+ channel assembly. *Neuron* **11**, 67-76.

Simon, A. M. and Goodenough, D. A. (1998). Diverse functions of vertebrate gap junctions. *Trends Cell Biol.* **8**, 477-483.

Skerrett, I. M., Aronowitz, J., Shin, J. H., Cymes, G., Kasperek, E., Cao, F. L. and Nicholson, B. J. (2002). Identification of amino acid residues lining the pore of a gap junction channel. *J. Cell Biol.* **159**, 349-360.

Stauffer, K. A. (1995). The gap junction proteins beta 1-connexin (connexin-32) and beta 2-connexin (connexin-26) can form heteromeric hemichannels. *J. Biol. Chem.* **270**, 6768-6772.

Steinberg, T. H., Civitelli, R., Geist, S. T., Robertson, A. J., Hick, E., Veenstra, R. D., Wang, H. Z., Warlow, P. M., Westphale, E. M. and Laing, J. G. (1994). Connexin43 and connexin45 form gap junctions with different molecular permeabilities in osteoblastic cells. *EMBO J.* **13**, 744-750.

Taylor, P. M., Thomas, P., Gorrie, G. H., Connolly, C. N., Smart, T. G. and Moss, S. J. (1999). Identification of amino acid residues within GABA(A) receptor beta subunits that mediate both homomeric and heteromeric receptor expression. *J. Neurosci.* **19**, 6360-6371.

Unger, V. M., Kumar, N. M., Gilula, N. B. and Yeager, M. (1999). Three-dimensional structure of a recombinant gap junction membrane channel. *Science* **283**, 1176-1180.

Valiunas, V., Gemel, J., Brink, P. R. and Beyer, E. C. (2001). Gap junction channels formed by coexpressed connexin40 and connexin43. *Am. J. Physiol. Heart Circ. Physiol.* **281**, H1675-H1689.

Veenstra, R. D. (1996). Size and selectivity of gap junction channels formed from different connexins. *J. Bioenerg. Biomembr.* **28**, 327-337.

Verrall, S. and Hall, Z. W. (1992). The N-terminal domains of acetylcholine receptor subunits contain recognition signals for the initial steps of receptor assembly. *Cell* **68**, 23-31.

Wang, X. G. and Peracchia, C. (1998). Molecular dissection of a basic COOH-terminal domain of Cx32 that inhibits gap junction gating sensitivity. *Am. J. Physiol.* **275**, C1384-C1390.

White, T. W. and Bruzzone, R. (1996). Multiple connexin proteins in single intercellular channels: connexin compatibility and functional consequences. *J. Bioenerg. Biomembr.* **28**, 339-350.

White, T. W. and Paul, D. L. (1999). Genetic diseases and gene knockouts reveal diverse connexin functions. *Annu. Rev. Physiol.* **61**, 283-310.

Willecke, K., Eiberger, J., Degen, J., Eckardt, D., Romualdi, A., Gueldenangel, M., Deutsch, U. and Sohl, G. (2002). Structural and functional diversity of connexin genes in the mouse and human genome. *Biol. Chem.* **383**, 725-737.

Yum, S. W., Kleopa, K. A., Shumas, S. and Scherer, S. S. (2002). Diverse trafficking abnormalities of Connexin32 mutants causing CMTX. *Neurobiol. Dis.* **11**, 43-52.

Zimmer, D. B., Green, C. R., Evans, W. H. and Gilula, N. B. (1987). Topological analysis of the major protein in isolated intact rat liver gap junctions and gap junction-derived single membrane structures. *J. Biol. Chem.* **262**, 7751-7763.